neighbouring cycles on each side. The derivative and instantaneous firing rate were estimated as the slope of the fit line, and its intercept in the central cycle. Circular ANOVA was performed using the test statistic $\sum \cos(\theta_i - \bar{\theta}_{g(i)})$, where $\bar{\theta}_{g(i)}$ is the circular mean for the group to which observation i is assigned. The null distribution was computed by 1,000-fold random reassignment of groups.

Computational simulations were performed in NEURON (http://www.neuron.yale.edu) using a two-compartment model of a hippocampal pyramidal cell. Conductance and calcium dynamics were as described by Migliore[22]. Compartment geometry: soma length 50 μm, diameter 40 μm, dendrite length 50 μm, diameter 3.3 μm. Somatic peak channel conductances (S cm^{-2}): G_{Na} 0.015; G_K(DR) (delayed rectifier) 0.009; G_K(A) (A-type) 0.0001; G_K(M) (M-type) 0.00002; G_K(AHP) (after-hyperpolarization) 0.004; G_{Ca}(L) (L-type) 0.0025; G_{Ca}(N) (N-type) 0.0025; G_{Ca}(T) (T-type) 0.00025; dendritic same without G_{Na}. 10-Hz sinusoidal conductances were added to the soma (Cl^-, peak 20 nS at 120°, phase modulation 50%) and dendrite (Na^+, peak 15 nS at 180°, phase modulation 30%). Modulation depth and preferred phase were based on extracellular recordings of interneurons and pyramidal cells *in vivo*[20]. The dendritic current was further modulated by a gaussian function of time (width 500 ms). Synaptic noise was added at the dendrite (Na^+, Poisson process, mean rate 1 kHz, peak conductance 5 nS).

Received 8 November 2001; accepted 2 April 2002; doi:10.1038/nature00808.

1. Singer, W. Synchronization of cortical activity and its putative role in information processing and learning. *Annu. Rev. Physiol.* **55,** 349–374 (1993).
2. O'Keefe, J. & Recce, M. L. Phase relationship between hippocampal place units and the EEG theta rhythm. *Hippocampus* **3,** 317–330 (1993).
3. Skaggs, W. E., McNaughton, B. L., Wilson, M. A. & Barnes, C. A. Theta phase precession in hippocampal neuronal populations and the compression of temporal sequences. *Hippocampus* **6,** 149–172 (1996).
4. Magee, J. C. Dendritic mechanisms of phase precession in hippocampal CA1 pyramidal neurons. *J. Neurophysiol.* **86,** 528–532 (2001).
5. Kamondi, A., Acsady, L., Wang, X. J. & Buzsaki, G. Theta oscillations in somata and dendrites of hippocampal pyramidal cells in vivo: activity-dependent phase-precession of action potentials. *Hippocampus* **8,** 244–261 (1998).
6. Adrian, E. D. & Zotterman, Y. The impulses produced by sensory nerve endings. Part 2. The response of a single end organ. *J. Physiol. (Lond.)* **61,** 151–171 (1926).
7. Gray, C. M. & Singer, W. Stimulus-specific neuronal oscillations in orientation columns of cat visual cortex. *Proc. Natl Acad. Sci. USA* **86,** 1698–1702 (1989).
8. Hopfield, J. J. Pattern recognition computation using action potential timing for stimulus representation. *Nature* **376,** 33–36 (1995).
9. Buzsaki, G. & Chrobak, J. J. Temporal structure in spatially organized neuronal ensembles: a role for interneuronal networks. *Curr. Opin. Neurobiol.* **5,** 504–510 (1995).
10. Vaadia, E. *et al.* Dynamics of neuronal interactions in monkey cortex in relation to behavioural events. *Nature* **373,** 515–518 (1995).
11. Riehle, A., Grun, S., Diesmann, M. & Aertsen, A. Spike synchronization and rate modulation differentially involved in motor cortical function. *Science* **278,** 1950–1953 (1997).
12. O'Keefe, J. & Nadel, L. *The Hippocampus as a Cognitive Map* (Clarendon, Oxford, 1978).
13. Burgess, N., Recce, M. & O'Keefe, J. A model of hippocampal function. *Neural Networks* **7,** 1065–1081 (1994).
14. Quirk, M. C., Blum, K. I. & Wilson, M. A. Experience-dependent changes in extracellular spike amplitude may reflect regulation of dendritic action potential back-propagation in rat hippocampal pyramidal cells. *J. Neurosci.* **21,** 240–248 (2001).
15. Harris, K. D., Hirase, H., Leinekugel, X., Henze, D. A. & Buzsaki, G. Temporal interaction between single spikes and complex spike bursts in hippocampal pyramidal cells. *Neuron* **32,** 141–149 (2001).
16. Hirase, H., Czurko, A., Csicsvari, J. & Buzsaki, G. Firing rate and theta-phase coding by hippocampal pyramidal neurons during 'space clamping'. *Eur. J. Neurosci.* **11,** 4373–4380 (1999).
17. Csicsvari, J., Hirase, H., Mamiya, A. & Buzsaki, G. Ensemble patterns of hippocampal CA3-CA1 neurons during sharp wave-associated population events. *Neuron* **28,** 585–594 (2000).
18. Csicsvari, J., Hirase, H., Czurko, A. & Buzsaki, G. Reliability and state dependence of pyramidal cell-interneuron synapses in the hippocampus: an ensemble approach in the behaving rat. *Neuron* **21,** 179–189 (1998).
19. Harris, K. D., Henze, D. A., Csicsvari, J., Hirase, H. & Buzsaki, G. Accuracy of tetrode spike separation as determined by simultaneous intracellular and extracellular measurements. *J. Neurophysiol.* **84,** 401–414 (2000).
20. Csicsvari, J., Hirase, H., Czurko, A., Mamiya, A. & Buzsaki, G. Oscillatory coupling of hippocampal pyramidal cells and interneurons in the behaving rat. *J. Neurosci.* **19,** 274–287 (1999).
21. Henze, D. A. & Buzsaki, G. Action potential threshold of hippocampal pyramidal cells in vivo is increased by recent spiking activity. *Neuroscience* **105,** 121–130 (2001).
22. Migliore, M., Cook, E. P., Jaffe, D. B., Turner, D. A. & Johnston, D. Computer simulations of morphologically reconstructed CA3 hippocampal neurons. *J. Neurophysiol.* **73,** 1157–1168 (1995).
23. Fisher, N. I. *Statistical Analysis of Circular Data* (Cambridge Univ. Press, New York, 1993).

Supplementary Information accompanies the paper on *Nature*'s website (http://www.nature.com/nature).

Acknowledgements

This work was supported by the NIH and the Human Frontier Science Program.

Competing interests statement

The authors declare that they have no competing financial interests.

Correspondence and requests for materials should be addressed to G.B. (e-mail: buzsaki@axon.rutgers.edu).

Role of experience and oscillations in transforming a rate code into a temporal code

M. R. Mehta, A. K. Lee & M. A. Wilson

Center for Learning & Memory, Department of Brain & Cognitive Sciences, RIKEN-MIT Neuroscience Research Center, Massachusetts Institute of Technology, Cambridge, Massachusetts 02139, USA

In the vast majority of brain areas, the firing rates of neurons, averaged over several hundred milliseconds to several seconds, can be strongly modulated by, and provide accurate information about, properties of their inputs. This is referred to as the rate code. However, the biophysical laws of synaptic plasticity require precise timing of spikes over short timescales (<10 ms)[1,2]. Hence it is critical to understand the physiological mechanisms that can generate precise spike timing *in vivo*, and the relationship between such a temporal code and a rate code. Here we propose a mechanism by which a temporal code can be generated through an interaction between an asymmetric rate code and oscillatory inhibition. Consistent with the predictions of our model, the rate[3,4] and temporal[5–7] codes of hippocampal pyramidal neurons are highly correlated. Furthermore, the temporal code becomes more robust with experience. The resulting spike timing satisfies the temporal order constraints of hebbian learning. Thus, oscillations and receptive field asymmetry may have a critical role in temporal sequence learning.

We recorded the activity of pyramidal neurons from the dorsal CA1 region of the hippocampus in awake, behaving rats (see Methods). The firing rate of these neurons depends on the spatial location of the rat[3], and hence these neurons are referred to as 'place cells'. The mean firing rates (averaged over >200 ms) of about 100 neurons can provide an accurate estimate of the rat's spatial location[4]. This is the hippocampal rate code.

In addition to this spatial parameter, hippocampal activity during active exploration is strongly modulated by a temporal parameter, namely the 8-Hz theta rhythm. In a classic study, O'Keefe and Recce showed that[5,6] the phase of the theta rhythm at which a place cell fires a spike steadily precesses to lower values as the rat moves further along the place field (Fig. 1a). Consistent with this, phase was highly (negatively) correlated with position ($r = -0.50 \pm 0.01$, $P < 0.0001$) across 171 recorded place fields (henceforth referred to as the 'population'). Normalizing by occupancy (see Methods) yields the firing rate as a function of position and phase—that is, the spatio-temporal receptive field (STRF, Fig. 1b). The firing rate increases as phase decreases (from 360° to 180°) and position increases, reaching a maximal value at a position beyond the centre (white line) of the place field and at 200° (red arrow) towards the end of the place field: that is, the firing rate is an inseparable function of high phases (180° < phase < 360°) and position. The firing rate at low phases (0° < phase < 180°) shows a weaker dependence on phase and position.

The vast majority of neurons have a similar spatio-temporal structure (as Fig. 1b), in which the firing rate shows a significant increase as the mean phase decreases and the distance within the place field increases (population average, Fig. 1c, d). Thus, there is spatial information in the precise timing of spikes (accurate up to 10 ms) with respect to the theta rhythm[5–7]. This is the hippocampal temporal code, which has several advantages over the rate code, such as insensitivity to the rat's running speed[5] and scale invariance[7].

Several computational models have been proposed to explain the origin of this temporal code[5,8–11]. These models were based upon the

observation that whereas the place field firing rate is a symmetric function of position, phase is not, suggesting that phase and rate are governed by separate mechanisms. However, recent results have demonstrated that place fields become asymmetric in an experience-dependent fashion[12], raising the possibility that rate and phase codes may be more directly coupled. Place field firing rate distributions in the present study were also asymmetric (skewness, -0.42 ± 0.05; $P < 0.0001$), such that the firing rate was low at the beginning of a place field, but was high at the end. On the basis of this observation we sought to test a hypothesized mechanism of the origin of the temporal code (Fig. 2), in which CA1 neurons receive theta rhythmic inhibitory input[13], as well as asymmetric excitatory input[12,14,15]. Under this model, the relationship between phase and rate is established by assuming that at the beginning of a place field excitation is low, and hence the latency with which a neuron comes out of inhibition and fires a spike, that is, spike phase, is high (360°). As the rat moves further along the place field, excitation increases, resulting in shorter latency to spiking (smaller phases), and higher rates. Such a mechanism, when applied to groups of overlapping place cells, will faithfully reproduce the temporal order of activation of place cells on short (<10 ms) timescales.

This mechanism makes the basic prediction that regions of high firing rate should have a lower mean phase, and vice versa. Indeed, mean phase was negatively correlated with mean firing rate both for individual cells (Fig. 3a, b) and across the population of neurons (Fig. 3c).

A second prediction of the model is that as the excitatory input increases with distance along the place field, the fraction of theta cycle during which excitation exceeds inhibition will also increase (blue bars, Fig. 2a), resulting in a wider phase distribution. Consistent with this prediction, we found an increase in the width of the phase distribution as a function of both distance (Fig. 3a, d) and rate ($r = 0.13 \pm 0.02$, $P < 0.0001$). Thus the temporal code was highly asymmetric, becoming less precise as the rat's position in the place field increased.

Further, excitation would be an increasing function of position in the first half of the place field, but initially increasing and then slightly decreasing function of position in the last half (Fig. 2). This predicts that the phase will be a more consistently decreasing function of position in the first half of the place field, compared to the last half. Thus the temporal code should be more robust in the first half of the place field than in the last half. Consistent with this, for the cell in Fig. 3a the phase is 6.2 times more strongly correlated with distance for spikes in the first half of the place field, compared with spikes in the last half of the place field. Similar results were true for the population of cells (Fig. 3e).

If the theta rhythm is purely sinusoidal, increasing levels of excitation will result in phase advancement from 360° at the trough of the theta cycle to 180° at the peak of the theta cycle. Beyond this point, the excitation exceeds inhibition throughout the theta cycle, resulting in a broader distribution of spikes. Thus, according to this model, the high phases should be more strongly correlated with

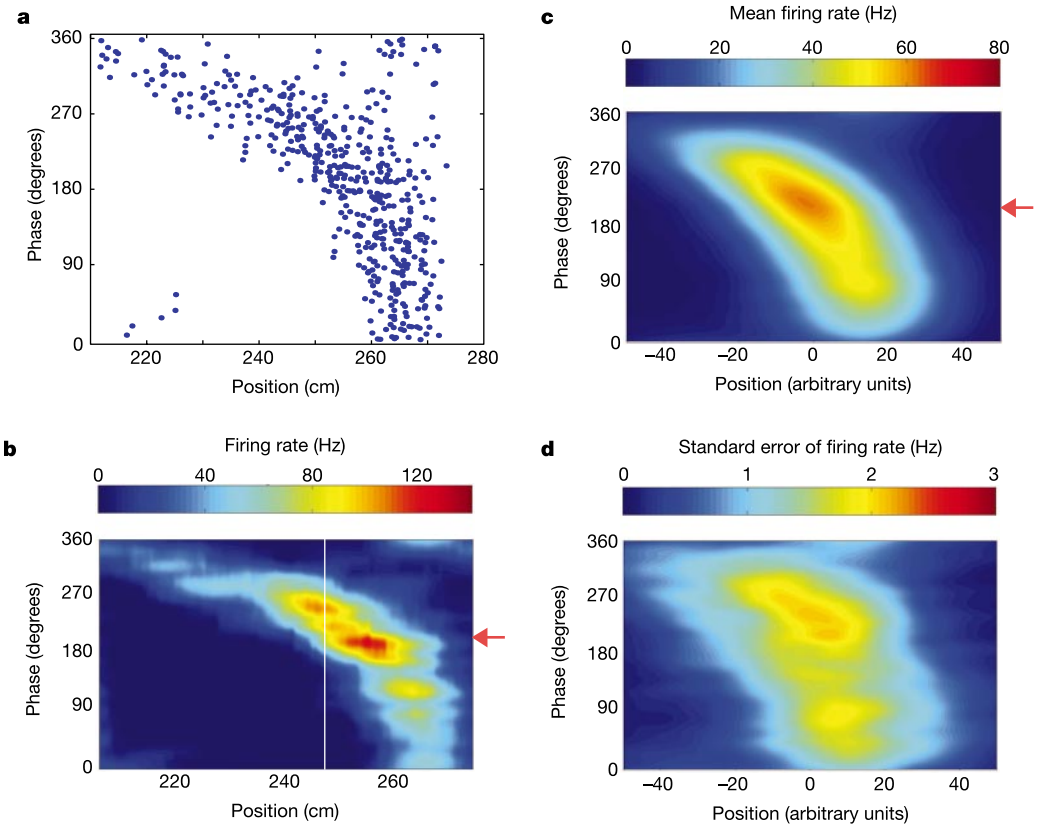

Figure 1 Hippocampal spatio-temporal receptive fields. **a**, The rat ran from left to right. Each point represents the phase of the theta rhythm (see Methods) and the rat's position at the time of occurrence of a spike from an isolated CA1 pyramidal neuron. Phase is highly correlated with position ($r = -0.8$). **b**, The firing rate for the neuron in **a** plotted as a function of position and phase (the spatio-temporal receptive field, STRF; see Methods). The centre of the place field (247 cm) is indicated by a white line. Phase (200°) corresponding to maximal firing rate is indicated by a red arrow. **c**, Population-averaged STRF. Each place field was re-scaled to be 100 pixels (66 cm) wide. The centres of the re-scaled STRFs were aligned at the origin. The average value of firing rate in each spatio-temporal bin is plotted. Phase (220°) corresponding to maximal firing rate is indicated by a red arrow. **d**. The standard error of firing rate was computed for the re-scaled population-averaged STRF (**c**), and plotted as a function of phase and position, showing that the firing rate modulations in **c** are highly significant.

position than the low phases. Indeed, the spikes at high phases for the cell in Fig. 3a are 7.4 times more strongly correlated with position than spikes at low phases. As a population, the correlation with position was 2.5 times stronger for high phases than low phases (Fig. 3f). The residual precession at low phases could arise because the theta rhythm is not purely sinusoidal[16].

The above results describe phase precession under the condition of an asymmetric receptive field. However, previous work has shown that place fields do not have a clear asymmetry during early exposure to an environment (Fig. 2b)[12]. In this condition, the rate will not be an increasing function of space, and hence phase will be poorly correlated with position. Thus, if the phase was indeed determined by the above mechanism, the temporal code should be less robust during this early period of exposure (Fig. 4a). Consistent with this prediction, we found that on average the population of place cells had a 2.1 times stronger correlation of phase with position after experience, compared to before (Fig. 4b, $P < 0.0001$). The time course of this evolution of the temporal code was also comparable to the time course of evolution of place field firing rate asymmetry[12].

In order to infer the precise effect of experience on firing rate as a function of position and phase, we computed the population-averaged STRF (Fig. 1c) for each lap. The resulting STRF shows a significant 2.2 times stronger correlation ($P < 0.00001$, paired t-test) of phase with position later during experience (sixteenth lap, Fig. 4d) than earlier (first lap, Fig. 4c). Whereas the correlation between firing rate and position, and between phase and position, becomes stronger with experience, the model predicts that there should be no change in the correlation between rate and phase. Consistent with this, the rate and phase were significantly correlated in both the first ($r = -0.10 \pm 0.03$, $P < 0.01$) and the sixteenth ($r = -0.07 \pm 0.03$, $P < 0.01$) laps, and there was no significant change in this correlation with experience ($P > 0.8$).

In three out of seven sessions, the rat's running velocity showed a significant change with experience (see Supplementary Information). Hence, we restricted the analysis to 67 place fields obtained from the remainder of four sessions where there was no significant change in the rat's running velocity throughout the first seventeen laps. The magnitude and time course of the experience dependence of the temporal code in these restricted data were virtually identical (see Supplementary Information) with the results presented in Fig. 4b. Thus the lap-specific changes in the temporal code could not arise from changes in the rat's behaviour.

Finally, if the phase precession is indeed restricted to mostly high phase spikes and is a result of the asymmetric nature of the firing rate distribution, the lap-by-lap fluctuation in these two parameters should be correlated. Indeed, averaged across the population, the firing rate asymmetry in a given lap was highly significantly correlated with the correlation of high phase spikes with position ($r = 0.13 \pm 0.02$, $P < 0.0001$).

Thus, our model suggests that the phase of spikes at a given location is largely determined by the net excitatory input at that location: a CA1 pyramidal neuron fires a spike when feed-forward excitation exceeds periodic inhibition. This simple mechanism would be modified in the presence of recurrent inhibition as follows. A pyramidal neuronal spike would activate recurrent inhibition within CA1, resulting in a suppression of subsequent pyramidal neuronal activity in that theta cycle. The suppression would have two complementary effects on the rate and the temporal codes. First, the pyramidal activity would be restricted to a small part of the theta cycle, thereby making the temporal code sharper. Second, the suppression would be strongest at higher rates, found towards the end of the place field. Therefore, the firing rate asymmetry would provide an underestimate of the asymmetry of the excitatory drive on a pyramidal neuron. Hence, the spike phase would become a better estimator than spike rate of the strength of feed-forward

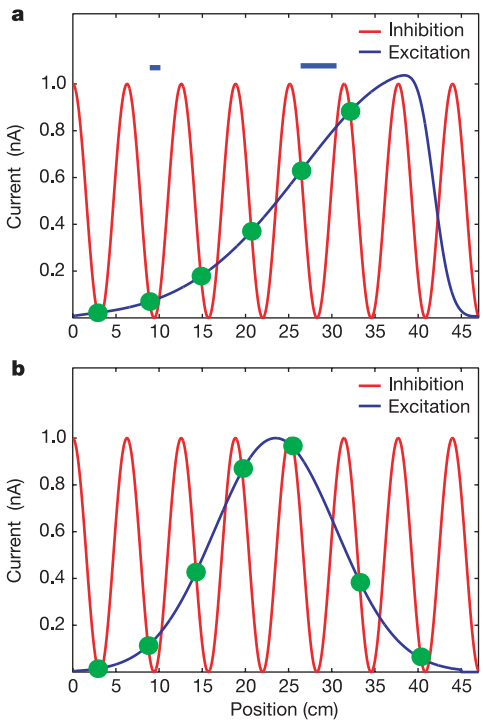

Figure 2 A mechanism that can generate a temporal code from a rate code. **a**, Each CA1 cell receives an asymmetric excitatory input (blue curve[12]) and periodic inhibitory input (red curve). The minima of inhibition correspond to 0° or 360°, and the maxima to 180°. The neuron will commence firing only when the excitation exceeds inhibition (green dots). Recurrent inhibition would then quickly terminate the activity. As the rat moves deeper into the place field, the excitation increases, phase decreases, and the neuron is active for a larger fraction of the theta cycle (blue bars) **b**, Before experience, the excitatory inputs to the CA1 neuron do not have a significant asymmetry (blue curve[12], this does not necessarily mean that individual place fields are symmetric). Therefore, the firing rate, and hence the phase, will be poorly correlated with position.

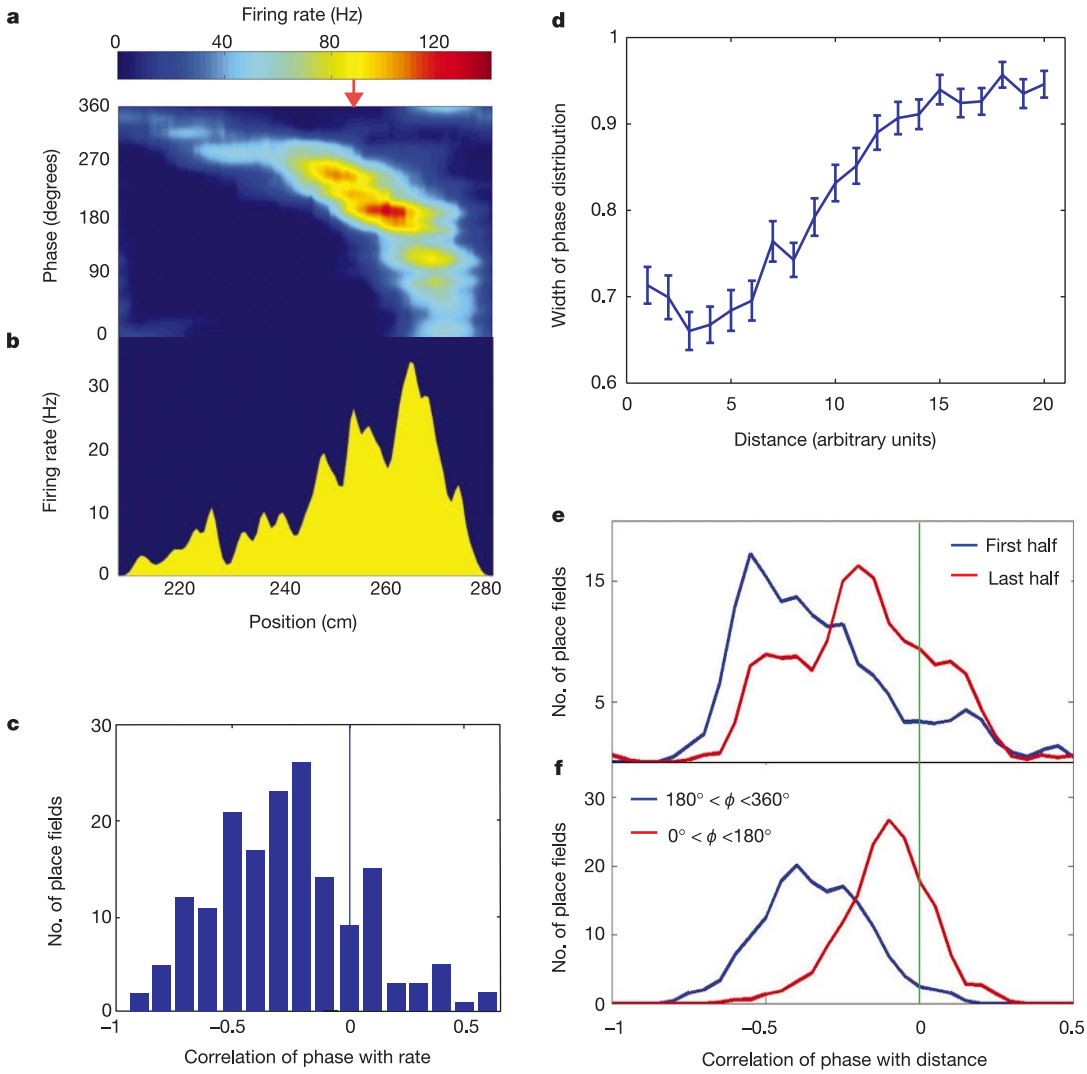

Figure 3 Relationship between hippocampal rate and temporal codes. The mean phase at a spatial location (**a**) is highly correlated with the mean firing rate (**b**) at that spatial location ($r = -0.6$). The place field centre is indicated by a red arrow. **c**, A histogram of correlation between rate and phase (see Methods) for the population of 171 cells shows that phase is negatively correlated with rate ($r = -0.30 \pm 0.02$, $P < 0.0001$). **d**, The width of phase distribution is larger at the end than at the beginning of the place field. Population-averaged value of the correlation of width of the phase distribution with position was $r = 0.50 \pm 0.03$, $P < 0.0001$. **e**, Histograms of correlation of phase with position in the first half of the place field (blue line, $r = -0.33 \pm 0.02$) is 1.7 times stronger than that in the last half (red line, $r = -0.20 \pm 0.02$, $P < 0.0001$). **f**, Histograms of correlation of spikes at high phases ($\phi = 180$–$360°$, blue line) and low phases ($\phi = 0$–$180°$, red line). The high phases are 2.5 times more correlated with position ($r = -0.34 \pm 0.01$) than the low phases ($r = -0.13 \pm 0.01$, $P < 0.0001$).

excitation and hence of the rat's spatial location. This could explain the observed stronger correlation between phase and position than between phase and rate, and the stronger correlation between phase and position than between rate and position. This model does not explicitly incorporate other elements of the hippocampal system, and hence it does not rule out the potential contribution of other sequence-retrieval-based models of phase precession[8,9,17,18].

Although previous experimental studies of place fields on linear tracks[5,6] did not explicitly investigate a relationship between the rate and phase, our results are in broad agreement with previous work[19] on a non-spatial wheel running task where the mean firing rate of a cell was negatively correlated with the mean phase of that cell. Recent experiments have suggested that NMDA (*N*-methyl-D-aspartate) antagonists do not eliminate phase precession. These experiments showed an increased rate of phase precession[20] with NMDA antagonists, which is consistent with our data (larger rate of precession before experience than after). The lack of direct measurement of the asymmetry of individual place fields and the correlation of phase with position and with rate in that study prevents direct comparison of their data with our model.

Recent *in vitro* experiments have shown that increasing amounts of current injection, coupled with theta-like oscillations, indeed result in phase advancement[21]. Consistent with our results[12,14], these *in vitro* experiments also obtained a clear relationship between the amplitude of injected current and phase in only a restricted part of the phase space. A similar relationship between rate and latency has also been observed in the STRF of direction selective neurons in V1 (see ref. 22 for a recent review), suggesting that similar mechanisms may be involved[12,14,15,23,24]. The phase coding of orientation selectivity[25] can also be explained by a similar mechanism. An optimally oriented bar would excite a cell maximally, resulting in spiking at the peaks of the gamma rhythm, whereas a sub-optimally tuned bar would correspond to lesser excitatory drive, resulting in a phase lag.

In its most general form, our model suggests that when a stimulus

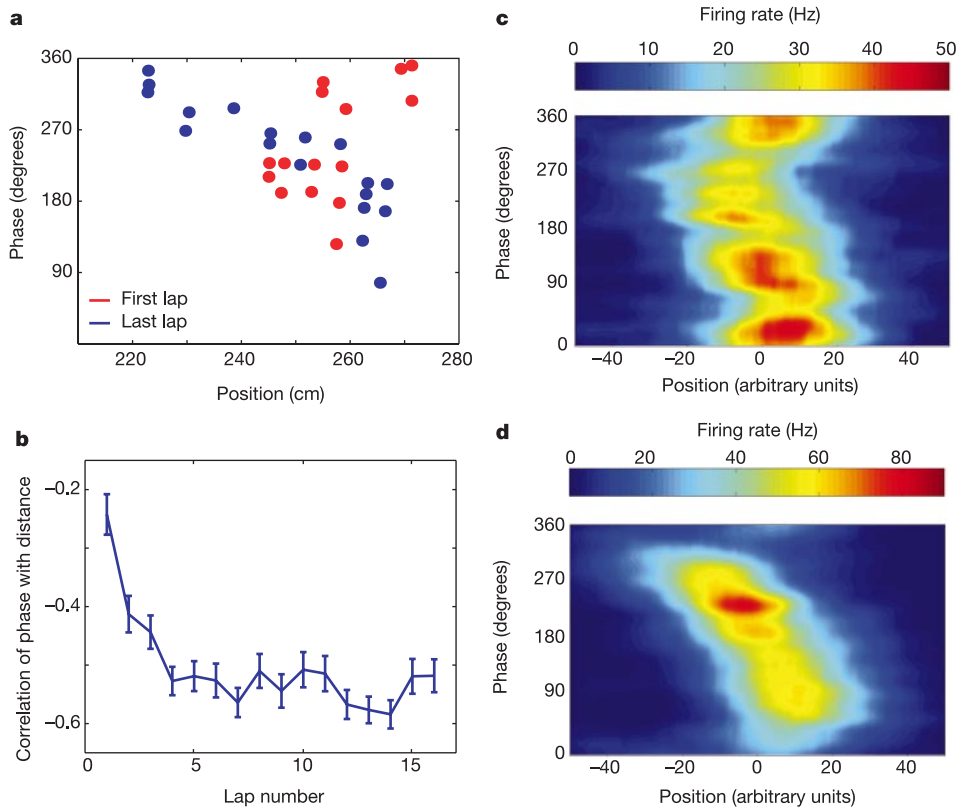

Figure 4 Experience dependence of the temporal code. **a**, All the spikes fired by a neuron (same as in Fig. 1a) during the first lap (red dots) through the place field and during the last (thirty-first) lap (blue dots). Although the phase is positively correlated with position in the first lap ($r = 0.6$), it is more strongly and negatively correlated with position after experience ($r = -0.9$). **b**, Correlation of phase with position was calculated for each cell for each lap in which the cell fired more than two spikes. The mean value of the correlation of phase with position, averaged across the population of place cells, is plotted as a function of experience. The phase is 2.1 times more strongly correlated with position in the sixteenth lap (mean $r = -0.50$) compared to the first lap (mean $r = -0.24$, $P < 0.0001$). **c**, **d**, Population-averaged STRF (see Methods) is plotted for the first lap (**c**) and the sixteenth lap (**d**). The mean phase is 2 times more strongly correlated with position in the sixteenth lap than in the first lap, and the mean phase is larger. The mean value of the phase of all the spikes in a given lap increased with experience from 171° before experience to 185° after experience, and the distribution of phases became wider with experience.

is turned on, the latency to first spike fired by a neuron would be inversely proportional to the subsequent firing rate of the neuron. Thus the latency of the first spike could provide rapid information about the stimulus. In the presence of oscillations this information would be repeated in each cycle.

One of the critical tasks of the central nervous system is to learn the causal relationships between events[12,15,26,27]. For example, spatial navigation may require formation of memory for the temporal order of activation of spatially selective cells[12,15,27–29]. But whereas the receptive fields are activated in a given sequence on a behaviourally relevant timescale (>1,000 ms), the biophysical laws of plasticity[1,2] require that the same sequence of events be replayed on short (<10 ms) timescales. This will not occur consistently if the neurons fired purely in a rate-varying Poisson fashion. However, in the presence of oscillations and asymmetric excitation, two place cells that are sequentially activated several hundred milliseconds apart will be activated in the same temporal sequence within tens of milliseconds, resulting in a replay (that is, binding) of the sequence within one theta cycle, and hence rapid learning of temporal sequences.

Thus oscillations can transform an asymmetric rate code into a temporal code. This can have a critical role in temporal sequence learning by compressing and replaying the behaviourally relevant temporal order of events occurring on long, physiological timescales into short timescales[5,6,27] relevant for synaptic plasticity. □

Methods

Three Long–Evans rats were trained to run on linear tracks (see refs 12 and 29 for details), and single unit data were recorded from the CA1 region of the dorsal hippocampus using tetrodes[12] according to NIH guidelines. Local field potentials (sampled at 2 kHz, filtered between 0.1 Hz and 900 Hz) and spike data (sampled at 31 kHz and filtered between 300 Hz to 9 kHz) were recorded from the same tetrodes in the pyramidal layer, along with the rat's position (spatial resolution 0.66 cm, sampling rate 30 Hz) and head direction. A total of 238 cells were active during behaviour, and were recorded in 3 rats in 7 sessions. Data from 158 of these cells were used in a previous study[12]. The tracks were 'linearized' for the purpose of analysis such that the distance increased along the rat's direction of motion through the place field. Data from goal locations were not used[12,29]. 171 place fields obtained from 140 place cells were used for the analyses.

The local field potential was bandpass-filtered off-line in the theta band (between 4 and 14 Hz), and the peaks and troughs of the theta rhythm were detected. Spike phase was computed with respect to the troughs of the filtered local field potential with the highest theta modulation (Fig. 2), with a phase offset that provided the highest correlation between phase and position[5]. A large proportion (82%) of neurons exhibited strongest phase precession with a negative phase offset (population average, −30°). All the subsequent analyses were carried out with respect to this ideal phase origin for each neuron.

Calculations involving mean and standard deviation of phases were done using circular statistics[30]. Thus, the value of width of a phase distribution[30] ranged between 0 and $\sqrt{2}$. Correlation of phase and position was computed using linear statistics. Mean values were computed over the entire population of 171 place fields, and their significance was estimated with Student's t-test. In order to compute the relationship between the rate and phase, spikes were arranged in ascending order of location. Mean position, mean rate, mean phase and the width of phase distribution, normalized by occupancy, were calculated for successive blocks of 5% of spikes. The last bin therefore had a variable number of spikes (between 0 and 5%) and hence was not used for the subsequent analyses. Relationships between these variables were obtained by computing the correlation coefficient across the blocks of data.

Hippocampal spatio-temporal receptive fields were computed by dividing the number

of spikes fired by a neuron in each spatio-temporal bin (spatial width 1 pixel = 0.66 cm, temporal width 1° ≈ 0.35 ms) by the total time spent by the rat in that bin. The result was smoothed by convolution with a two-dimensional gaussian (spatial width 2.4 cm, temporal width 12° ≈ 4.2 ms).

Received 24 October 2001; accepted 22 April 2002; doi:10.1038/nature00807.

1. Markram, H., Lubke, J., Frotscher, M. & Sakmann, B. Regulation of synaptic efficacy by coincidence of postsynaptic APs and EPSPs. *Science* **275,** 213–215 (1997).
2. Bi, G. Q. & Poo, M. M. Synaptic modifications in cultured hippocampal neurons: dependence on spike timing, synaptic strength, and postsynaptic cell type. *J. Neurosci.* **18,** 10464–10472 (1998).
3. O'Keefe, J. & Dostrovsky, J. The hippocampus as a spatial map. Preliminary evidence from unit activity in the freely-moving rat. *Brain Res.* **34,** 171–175 (1971).
4. Wilson, M. A. & McNaughton, B. L. Dynamics of the hippocampal ensemble code for space. *Science* **261,** 1055–1058 (1993).
5. O'Keefe, J. & Recce, M. L. Phase relationship between hippocampal place units and the EEG theta rhythm. *Hippocampus* **3,** 317–330 (1993).
6. Skaggs, W. E., McNaughton, B. L., Wilson, M. A. & Barnes, C. A. Theta phase precession in hippocampal neuronal populations and the compression of temporal sequences. *Hippocampus* **6,** 149–172 (1996).
7. Hopfield, J. J. Pattern recognition computation using action potential timing for stimulus representation. *Nature* **376,** 33–36 (1995).
8. Tsodyks, M. V., Skaggs, W. E., Sejnowski, T. J. & McNaughton, B. L. Population dynamics and theta rhythm phase precession of hippocampal place cell firing: a spiking neuron model. *Hippocampus* **6,** 271–280 (1996).
9. Wallenstein, G. V. & Hasselmo, M. E. GABAergic modulation of hippocampal population activity: sequence learning, place field development, and the phase precession effect. *J. Neurophysiol.* **78,** 393–408 (1997).
10. Kamondi, A., Acsady, L., Wang, X. J. & Buzsaki, G. Theta oscillations in somata and dendrites of hippocampal pyramidal cells in vivo: activity-dependent phase-precession of action potentials. *Hippocampus* **8,** 244–261 (1998).
11. Bose, A., Booth, V. & Recce, M. A temporal mechanism for generating the phase precession of hippocampal place cells. *J. Comput. Neurosci.* **9,** 5–30 (2000).
12. Mehta, M. R., Quirk, M. C. & Wilson, M. A. Experience-dependent asymmetric shape of hippocampal receptive fields. *Neuron* **25,** 707–715 (2000).
13. Toth, K., Freund, T. F. & Miles, R. Disinhibition of rat hippocampal pyramidal cells by GABAergic afferents from the septum. *J. Physiol.* **500,** 463–474 (1997).
14. Mehta, M. R. & Wilson, M. A. From hippocampus to V1: Effect of LTP on spatio-temporal dynamics of receptive fields. *Neurocomputing* **32,** 905–911 (2000).
15. Mehta, M. R. Neuronal dynamics of predictive coding. *Neuroscientist* **7,** 490–495 (2001).
16. Buzsaki, G., Rappelsberger, P. & Kellenyi, L. Depth profiles of hippocampal rhythmic slow activity ('theta rhythm') depend on behaviour. *Electroencephalogr. Clin. Neurophysiol.* **61,** 77–88 (1985).
17. Jensen, O. & Lisman, J. E. Hippocampal CA3 region predicts memory sequences: accounting for the phase precession of place cells. *Learn. Mem.* **3,** 279–287 (1996).
18. Hasselmo, M. E., Fransen, E., Dickson, C. & Alonso, A. A. Computational modeling of entorhinal cortex. *Ann. NY Acad. Sci.* **911,** 418–446 (2000).
19. Hirase, H., Czurko, H. H., Csicsvari, J. & Buzsaki, G. Firing rate and theta-phase coding by hippocampal pyramidal neurons during 'space clamping'. *Eur. J. Neurosci.* **11,** 4373–4380 (1999).
20. Ekstrom, A. D., Meltzer, J., McNaughton, B. L. & Barnes, C. A. NMDA receptor antagonism blocks experience-dependent expansion of hippocampal "place fields". *Neuron* **31,** 631–638 (2001).
21. Magee, J. C. Dendritic mechanisms of phase precession in hippocampal ca1 pyramidal neurons. *J. Neurophysiol.* **86,** 528–532 (2001).
22. Livingstone, M. S. Mechanisms of direction selectivity in macaque V1. *Neuron* **20,** 509–526 (1998).
23. Chance, F. S., Nelson, S. B. & Abbott, L. F. Synaptic depression and the temporal response characteristics of V1 cells. *J. Neurosci.* **18,** 4785–4799 (1998).
24. Rao, R. P. & Sejnowski, T. J. Predictive learning of temporal sequences in recurrent neocortical circuits. *Novartis Found. Symp.* **239,** 208–229 (2001).
25. Konig, P., Engel, A. K., Roelfsema, P. R. & Singer, W. How precise is neuronal synchronization? *Neural Comput.* **7,** 469–485 (1995).
26. Levy, W. B., in *Computational Models of Learning in Simple Neural Systems* (eds Hawkins, R. D. & Bower, J. H.) 243–305 (Academic, New York, 1989).
27. Blum, K. I. & Abbott, L. F. A model of spatial map formation in the hippocampus of the rat. *Neural Comput.* **8,** 85–93 (1996).
28. Mehta, M. R. & McNaughton, B. L. in *Computational Neuroscience: Trends in Research* (ed. Bower, J.) 741–745 (Plenum, New York, 1996).
29. Mehta, M. R., Barnes, C. A. & McNaughton, B. L. Experience-dependent, asymmetric expansion of hippocampal place fields. *Proc. Natl Acad. Sci. USA* **94,** 8918–8921 (1997).
30. Zar, J. H. *Biostatistical Analysis* (Prentice Hall, New Jersey, 1999).

Supplementary Information accompanies the paper on *Nature*'s website (http://www.nature.com/nature).

Acknowledgements

We thank W.F. Asaad, G. Liu, K. Louie, J. Raymond and S. Schnall for comments on the manuscript. This work was supported by the NIH (M.A.W.) and an HHMI pre-doctoral fellowship (A.K.L.). Parts of this work were presented at the Computational Neuroscience Meeting 2000 and at the Society for Neuroscience meeting 2001.

Competing interests statement

The authors declare that they have no competing financial interests.

Correspondence and requests for materials should be addressed to M.R.M. (e-mail: mayank@mit.edu) or M.A.W. (e-mail: wilson@cortical.mit.edu).

Modulation of virulence within a pathogenicity island in vancomycin-resistant *Enterococcus faecalis*

Nathan Shankar*, Arto S. Baghdayan* & Michael S. Gilmore†

** Department of Pharmaceutical Sciences and † Departments of Ophthalmology and Microbiology & Immunology, University of Oklahoma Health Sciences Center, PO Box 26901, Oklahoma City, Oklahoma 73190, USA*

Enterococci are members of the healthy human intestinal flora, but are also leading causes of highly antibiotic-resistant, hospital-acquired infection[1]. We examined the genomes of a strain of *Enterococcus faecalis* that caused an infectious outbreak in a hospital ward in the mid-1980s (ref. 2), and a strain that was identified as the first vancomycin-resistant isolate in the United States[3], and found that virulence determinants were clustered on a large pathogenicity island, a genetic element previously unknown in this genus. The pathogenicity island, which varies only subtly between strains, is approximately 150 kilobases in size, has a lower G + C content than the rest of the genome, and is flanked by terminal repeats. Here we show that subtle variations within the structure of the pathogenicity island enable strains harbouring the element to modulate virulence, and that these variations occur at high frequency. Moreover, the enterococcal pathogenicity island, in addition to coding for most known auxiliary traits that enhance virulence of the organism, includes a number of additional, previously unstudied genes that are rare in non-infection-derived isolates, identifying a class of new targets associated with disease which are not essential for the commensal behaviour of the organism.

In a study of a hospital ward epidemic in the mid-1980s, one *E. faecalis* strain resistant to many different antibiotics was identified as having caused over 30 infections (typified by isolate MMH594) and carried a fivefold increased risk of death within 3 weeks of isolation[2]. Several years later, the first vancomycin-resistant enterococcal isolate in the United States was identified approximately 400 miles away, and serial isolates (V583 and V586) were obtained from a chronically infected patient[3]. The vancomycin-resistance determinant has been characterized in molecular detail[4], and strain V583 was provided for genome analysis (for strain V583 genome data see http://www.tigr.org/tigr-scripts/CMR2/GenomePage3.spl?database = gef).

We and others have analysed a number of virulence factors in *E. faecalis*, including a structurally novel toxin, the cytolysin[5–7], and a surface protein, Esp[8], which contributes to colonization of the bladder in a model of urinary tract infection[9]. Esp confers biofilm production capability to enterococci[10], and a highly conserved Esp variant is common among clinical vancomycin-resistant and vancomycin-sensitive *E. faecium* strains[11–13]. *Enterococcus faecalis* strains V583 and V586 were isolated from a patient 11 days apart[3], and initial studies failed to identify differences between these isolates as they exhibited what appeared to be identical DNA fingerprint patterns. However, subsequent experiments designed to localize genes coding for both Esp and cytolysin found them on the chromosome of V586, but not V583. The difference was localized to a relatively small deletion within a roughly 315 kilobase (kb) *Sfi*I fragment in V583 (Fig. 1), which suggested that *cyl* and *esp* are closely linked.

Alignment and comparison of nucleotide sequences coding for the cytolysin operon, *esp* and surrounding regions of the V586 genome (Esp^+, Cyl^-), and the point of deletion of these functions in the genome of V583 (Esp^-, Cyl^-), (see http://www.tigr.org/tigr-scripts/CMR2/GenomePage3.spl?database = gef), revealed a